FROM THE DEPARTMENT OF PHYSICAL CELL RESEARCH AND THE DEPARTMENT OF PATHO-ANATOMY, KAROLINSKA INSTITUTET, STOCKHOLM 60

BIOPHYSICAL STUDIES ON BONE TISSUE

XII. *Experimentally produced ectopic bone tissue*

By

BENGT ENGFELDT and ARNE ENGSTRÖM

INTRODUCTION

The experimental production of ectopic bone has been described by several investigators. *Levander* (1938) obtained cartilage and bone in rabbit muscle by the injection of alcoholic extracts of bone tissue. He was of the opinion that the development of ectopic bone was due to some osteogenic substance in the extracts. Similar views have been expressed by other authors, see *Lacroix* (1951) for survey. It was shown, however, by *Heinen* et al. (1949) that ectopic bone could be produced in rabbits by the injection of alcohol alone.

The purpose of the present investigation is to study ectopic bone by biophysical methods and to discuss the findings in relation to normal bone tissue. A comparison between the ectopic bone and the bone tissue from a few cases of osteogenesis imperfecta will also be given.

MATERIAL

Injections of one to two ml of 40 % ethanol were made at several loci in the biceps and quadriceps of four young rabbits. After three months two macroscopic bone specimens, 5 mm in diameter were found at the sites of injection. In the other cases only hard scar tissue was observed. Thin sections (about 50 microns) of the ectopic bone were obtained by grinding. For this purpose the small pieces of ectopic bone were embedded in plastic (methylmethacrylate). For comparison longitudinal and transverse sections from the long bones of young rabbits were prepared by grinding. Sections of the bone from some cases of osteogenesis imperfecta were obtained in a similar way.

METHODS AND THEORETICAL CONSIDERATIONS

The distribution of mineral salts in the ground sections of the ectopic bone was studied by microradiography. In essentials the method described by *Engström* and *Wegstedt* (1951) was followed. For a general discussion on the use of x-ray methods in histochemistry see *Engström* (1953). For some of the experiments a Machlett OEG 50 x-ray tube was energized with 8 kV and emitted x-rays with short wavelength limit of 1.5 Å. In other cases the OEG 50 tube, which has a 0.2 mm thick Be-window, was run with 24 kV fully rectified D.C. and at

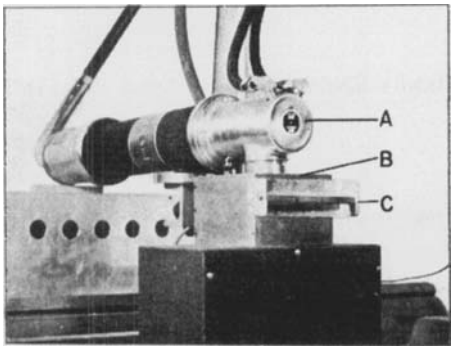

Fig. 1.
Arrangement for microradiography with Machlett OEG 50 x-ray tube. Inherent filtration 0.2 mm Be. Tungsten target. A, X-ray tube; B, Camera; C, Shutter for camera.

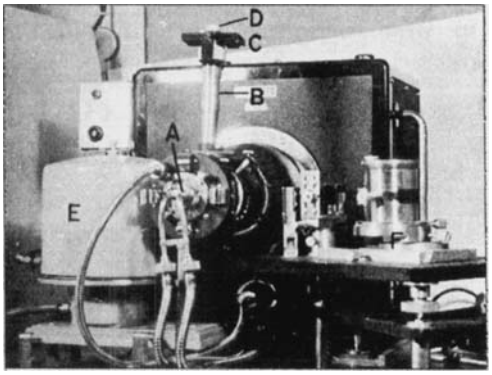

Fig. 2.
Equipment for stereomicroradiography and x-ray diffraction. A, X-ray tube, Cu-target; B, Extension tube for the stereomicrocamera, labelled C; D, fluorescent screen; E, 19 cm Hilger powder x-ray diffraction camera; F, Guinier camera for the registration of diffraction diagrams with monochromatic x-rays.

15 mA. Fig. 1. shows how the OEG 50 tube is arranged for microradiography. A stereomicroradiographic camera (Fig. 2) designed by *Müller* (Siemens Reinigerwerke Erlangen) was used for taking some of the microradiograms. This camera was attached to a Siemens Crystalloflex II x-ray unit. Both intact and decalcified sections were examined by microradiography. The decalcified sections were microradiographed with extremely soft x-rays (8 Å and longer wavelengths) in the apparatus described by *Engström* and *Lindström* 1949–1950. The microradiograms were recorded on Eastman Kodak Spectroscopic plate 649 which is a fine grained photographic emulsion, which can resolve more than 1000 lines per millimeter. The microradiograms of the bone sample which thus were recorded at unit magnification showed microscopic details. Enlarged images of the original microradiograms were obtained by photomicrography.

The following theoretical consideration shows that the intensity distribution in the microradiographic image of a thin ground section of bone can be interpreted in terms of distribution of the mineral salts. The absorption of monochromatic x-rays in matter follows the simple exponential law:

$$E = \ln \frac{I_0}{I} = \frac{\mu_1}{\rho_1} \cdot m_1 + \frac{\mu_2}{\rho_2} m_2 \ldots \frac{\mu_n}{\rho_n} m_n \ldots\ldots\ldots 1$$

In this equation the symbols have the following meaning

I_0 = intensity of the incident x-rays.
I = intensity of the transmitted x-rays.
E = extinction defined as $\ln \frac{I_0}{I}$.
μ = linear absorption coefficient, cm^{-1}.
ρ = density, $g \cdot cm^{-3}$.
m = weight of substance, $g \cdot cm^{-2}$.
$\frac{\mu}{\rho}$ = mass absorption coefficient, $g^{-1} \cdot cm^2$.

The sample is composed of several components 1, 2 ..... n. In the case of a thin ground section of bone tissue the x-ray absorption can be divided into two components, the inorganic and the organic.

Equation 1 therefore can be written:

$$E = \ln \frac{I_0}{I} = \frac{\mu_i}{\rho_i} \cdot m_i + \frac{\mu_0}{\rho_0} \cdot m_0 \ldots\ldots\ldots\ldots 2$$

where indices i and o stand for the inorganic and organic fraction respectively. The mass absorption coefficient $\left(\frac{\mu}{\rho}\right)$ increases with the increasing wavelength of the x-rays and also with the increasing atomic number of the absorber. At certain critical wavelengths, however, there occur abrupt changes in absorption, and these changes are called absorption edges or discontinuities. For example Ca has its shortest absorption edge (K-edge) at 3.3 Å., nitrogen has its k-edge at 31.4 Å. In general the position of the absorption edges of a given series (K, L, M, etc.) is shifted towards longer wavelengths with the decreasing atomic number of the absorber.

The mass absorption coefficient is composed of two terms:

$$\frac{\mu}{\rho} = \frac{\tau}{\rho} + \frac{\sigma}{\rho} \qquad \ldots\ldots\ldots\ldots\ldots\ldots\ldots\ldots\ldots\ldots\ldots\ldots\ 3$$

$\frac{\tau}{\rho}$ is the true protoelectric absorption coefficient and $\frac{\sigma}{\rho}$ the mass scattering coefficient. The value of $\frac{\tau}{\rho}$ is easy to calculate but the value for $\frac{\sigma}{\rho}$ which includes both modified and unmodified scattering, is more difficult to assess. However, it is only for very short x-rays and elements of low atomic numbers that $\frac{\sigma}{\rho}$ has to be taken into account. In the wavelength range used for historadiography of thin bone sections the values of $\frac{\tau}{\rho}$ are much greater than those for $\frac{\sigma}{\rho}$ and therefore at the experiments reported in this paper $\frac{\sigma}{\rho}$ can be neglected in comparison with $\frac{\tau}{\rho}$ (For details see *Engström* 1946).

For bone tissue the values of the mass absorption coefficient $\left(\frac{\mu}{\rho}\right)$ have been calculated for the inorganic fraction, apatite $[Ca_{10}(PO_4)_6(OH)_2]$, and for nitrogen which serves as a representative for the organic fraction. The numerical values of the mass absorption coefficient are given in Table 1.

The density of the apatite is about 3 and for the waterfree organic fraction the density is about 1,2. When the x-ray extinction for a

TABLE 1

Mass absorption coefficients for apatite (inorganic bone phase) and nitrogen (representing the organic bone phase) at various wavelengths.

Radiation		Mass absorption coefficient $cm^2 \cdot g^{-1}$	
λ Å	kV	$\frac{\mu}{\rho}$ apatite	$\frac{\mu}{\rho}$ org. (N)
0.5	24.6	~ 3.5	~ 0.4
1.0	12.3	26	2.1
1.5	8.3	81	7.7
2.0	6.2	178	19
2.5	4.9	330	29
3.0	4.1	545	57

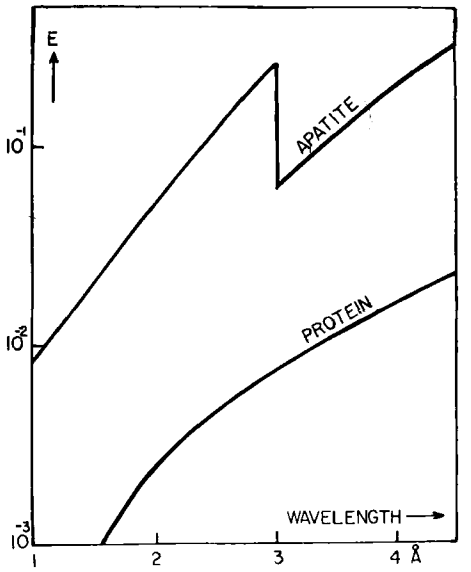

Fig. 3.

Extinction for x-rays of various wavelengths in 1 micron thick layers of apatite and protein.

1 micron thick layer for apatite and protein is calculated the results shown in figure 3 are obtained. The x-ray absorption of the protein fraction can be written:

$$E = \ln \frac{I_0}{I} = \frac{\mu}{\rho}\text{prot.} \cdot m_{\text{prot.}} \text{ which can be replaced}$$

(with negligible error) by

$$E = \ln \frac{I_0}{I} = \frac{\mu}{\rho} N \cdot m_{\text{prot.}}$$

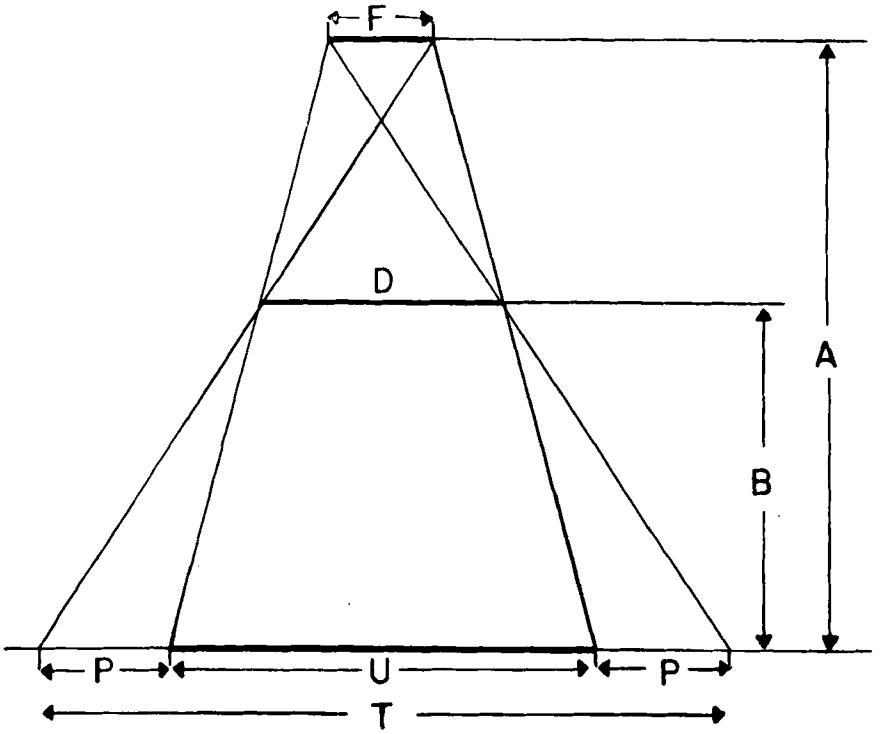

Fig. 4.

Geometry of x-ray image formation in microradiography. F, Focal spot on target; D, Diameter of sample; U, Umbra; P, Penumbra; T, Total shadow; A, Distance between the focal spot and the image plane; B, Distance between sample and image plane.

From the figure it is evident that for the wavelength range used, practically all absorption is due to the mineral salts and therefore the microradiograms registered under these conditions show the distribution of mineral salts.

One of the important factors for the image definition in the microradiogram is the geometry during the exposure. Since the focus of an x-ray tube consists of a surface, at least a part of the shadow (T) produced by the object consists of penumbra, P, (Fig. 4). The part of the shadow consisting of umbra, U, may generally be expressed as

$$U = \frac{AD - BF}{A - B}$$

where A is the distance from focus to image plane, B the distance from object to image plane, F the diameter of the focus and D the diameter of the object.

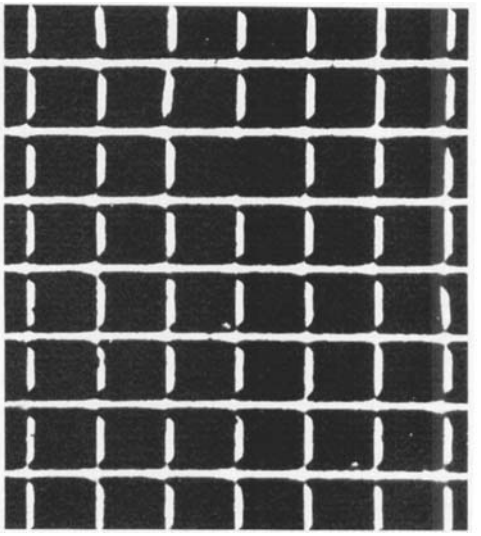

Fig. 5.
Resolution test of microradiographic procedure used. Microradiogram of silver grid. Each bar is 3 microns wide. The resolution is better than 0.5 micron. Voltage: 5 kV. Filter: 0.2 mm Be. Lippman film.

Differentiation with respect to B gives

$$\frac{dU}{dB} \quad \frac{A(D - F)}{(A - B)^2}$$

which for this discussion can be written,

$$\frac{dU}{dB} = (D - F)$$

If $D > F$; $\frac{dU}{dB} > 0$, U increases with B;

If $D = F$; $\frac{dU}{dB} = 0$, U is constant;

If $D < F$; $\frac{dU}{dB} < 0$, U decreases as B increases.

The dimension of the smallest object that gives an image with a certain relation to the size of the object is represented by $\frac{B}{A} \cdot F$.

The resolution of the microradiographic technique we used is highly satisfactory. Figure 5 shows an enlargement of a microradio-

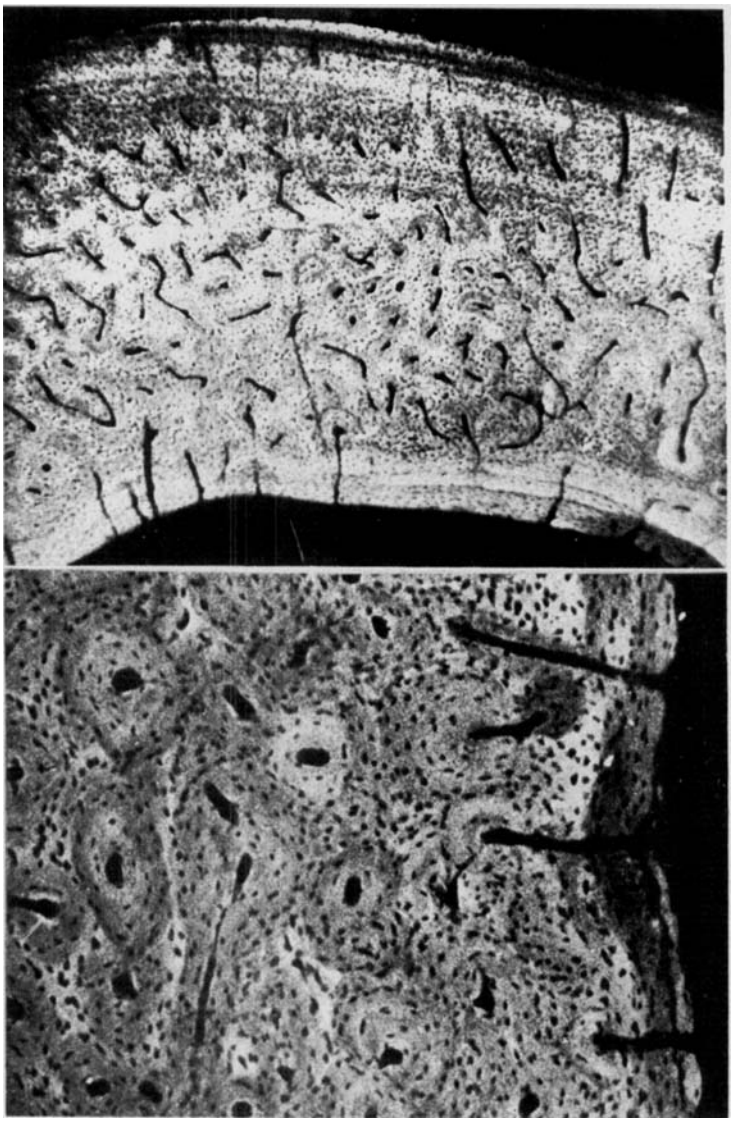

6 a

6 b

Fig. 6.

A. Microradiogram of a cross section of rabbit femur (diaphysis). The section was ground to a thickness of 50 microns. The varying degree of mineralization is well demonstrated. The whiter a structure appears in the picture, the higher its content of mineral salts.

B. A portion of Fig. 6 A at higher magnification. The osteocytes appear as x-ray transparent black dots. The lamellar structure of the osteons can be seen in the originals, indicating that the ratio organic to inorganic materials varies in the different lamellae. Voltage: 24 kV. Filter: 0.2 mm Be. Eastman Kodak Spectroscopic Plate 649.

gram of a silver grid (kindly supplied by Prof. V. E. Cosslett, Cambridge, England) in which the widest bars are 3 microns. It is clearly demonstrated that the x-ray technique has a resolution better than 0.5 micron in objects with good contrast and bone tissue is such an object.

The chemical nature of the mineral salts deposited in the ectopic bone tissue was studied by wide angle x-ray diffraction. Powdered

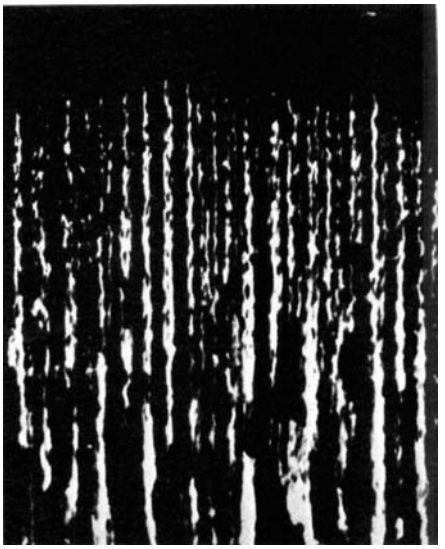

Fig. 7.
Microradiogram of a longitudinal section of the growth zone of metatarsus. The epiphyseal plate (at the top in the figure) shows no x-ray absorption and therefore contains no mineral salts. Voltage: 24 kV. Filter: 0.2 mm Be. Eastman Kodak Spectroscopic Plate 649.

ectopic bone was examined in Debye-Scherrer cameras having diameters of 57 mm and 190 mm. The latter camera (Hilger) was used for precision measurements of the lattice parameters. In order to study orientation of the mineral component in the ectopic bone the sections which had previously been microradiographed were examined in a *Chesley* (1947) microdiffraction camera.

After microradiography and micro x-ray diffraction the ground sections were decalcified, mounted in saline, and examined in polarized light in order to determine the orientation of the organic fibrillae.

The in vitro exchange of radioactive phosphate and radioactive calcium ($Ca^{45}Cl_2$) was studied by autoradiography. The ground sections were incubated for 15 and 36 hours in a solution containing the

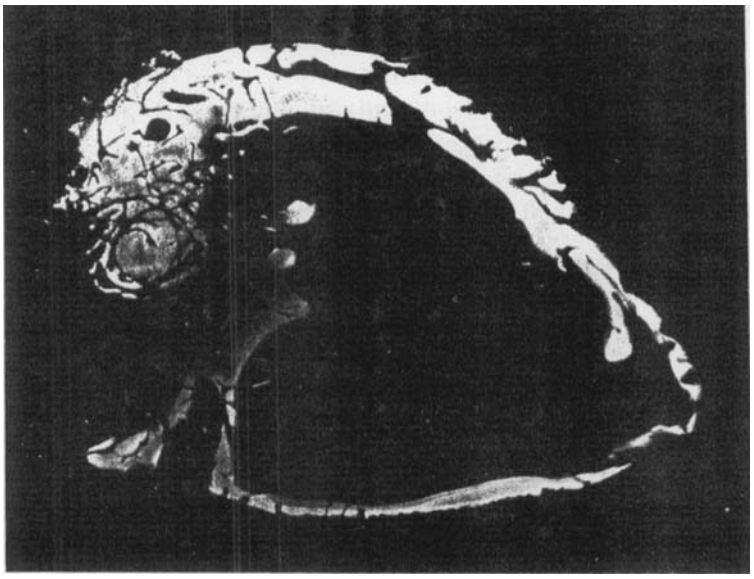

Fig. 8.
Ground section of ectopic bone. Microradiogram at low magnification. Note the spaces for the blood vessel network. Voltage: 8 kV. Filter: 0.2 mm Be. Lippmann-film.

isotope. The sections were then ground on both sides after the incubation. About 10 microns were removed on each side. Agfa Printon photographic emulsion was used to record the autoradiographic images which were enlarged by photomicrography.

RESULTS

Both transverse and longitudinal sections from the long bones of normal rabbits show an uneven mineralization. The microradiogram (Fig. 6 a) of a transverse section from the diaphysis of the femur reveals a bone tissue mainly composed of lamellar bone with a rather high degree of mineralization. The different lamellae are separated by thin highly mineralized lines running axially in the bone. In some areas resorption cavities are found and also haversian systems with varying content of mineral salts. The difference in mineralization between different structures is more evident in Fig. 6 b which shows an area in high manifestation with many haversian systems. The newly formed osteons which have a low content of minerals represent areas with recent deposition of mineral salts while with increasing age their degree of mineralization successively increases.

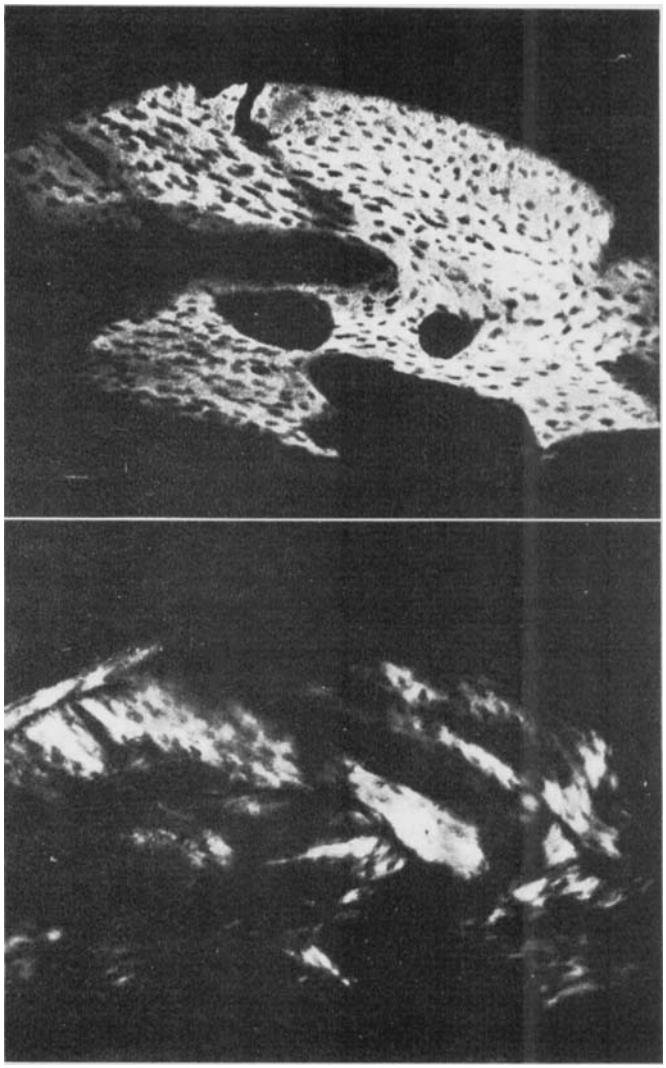

9a

9b

Fig. 9.

A. Microradiogram of ectopic bone at high magnification. Voltage: 8 kV. Filter: 0.2 mm Be. Lippmann-film.

B. The same section photographed in polarized light after decalcification.

A microradiogram of a longitudinal section from a long bone which is still growing is shown in Fig. 7. The cartilage in the epiphyseal plate does not show any significant x-ray absorption but in the metaphysis where the mineralization starts, thin bars of mineralized tissue running longitudinally can be seen. These bars which are getting wider

towards the diaphysis show an increasing absorption hence an increased mineralization in this direction.

The distribution of mineral salts in sections of the ectopic bone produced by alcohol injection in rabbits can be seen in the microradiograms shown in Figs. 8 and 9 a. The bone tissue shows a rather high and even mineralization and most of it has great similarities with lamellar bone. The vascularization is rich. At some sites structures with a low content of mineral salts are seen and sometimes these structures resemble haversian systems. Minor areas which show evid-

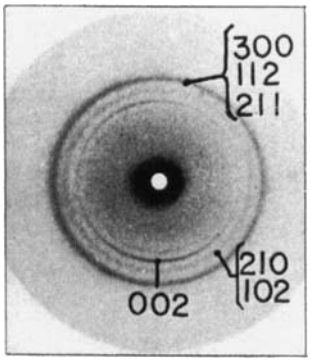

Fig. 10.
Flat film x-ray diffraction diagram of ectopic bone. Slight orientation is seen in the 002-reflection indicating some alignment of the crystallographic c-axes. Nickel-filtered Cu K-radiation. (1.54 Å).

ence of resorption are also found. In the microradiogram the cells appear as black, round to oval shaped spots which are not mineralized.

Decalcified sections show in polarized light a well organized fibre pattern with rather broad, but not especially long bundles running in somewhat different directions (Fig. 9 b). In transmitted light the bone tissue is seen to be moderately cellular and in some areas it has a coarse fibrillar structure.

The in vitro uptake of radioactive phosphate and calcium in the ectopic bone tissue takes place at several sites. It could be demonstrated that the major part of the labelling in vitro occurs in structures with a low degree of mineralization, which is in agreement with previous experiments.

Fig. 10 shows the x-ray diffraction of a part of the area from which the microradiogram (Fig. 9 a) was obtained. It is an apatite pattern, identical with that found in normal bone tissue. The 3.44 Å diffraction ring (002) is slightly oriented. A comparison between the

x-ray diffraction patterns and the decalcified section photographed in polarized light, indicated that the c-axis of the hexagonal apatite unit cell was almost parallel with the fiber axis of the fibrillae. In Fig. 11

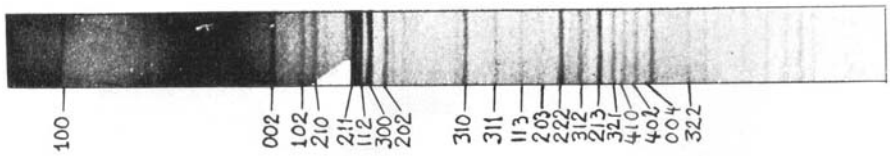

Fig. 11.

Powder diagram in 19 cm camera of ectopic bone heated to 600 C° for one hour. The diffraction lines are sharper than from unheated bone. This effect is due to the growth of the crystallites. The mark in the diagram is at an angle of 15°. The diagram is indexed at the basis of a hexagonal unit cell with the axes a = 9.41 and c = 6.87 Å. Nickelfiltered Cu K-radiation (1.54 Å).

is shown a pattern of heated ectopic bone. Precision measurement on this pattern gave the size of the unit cell to be a = 9.41 Å and c = 6.87 Å which values are also found in normal bone.

DISCUSSION

The bone tissue produced by the injection of alcohol into rabbit muscles has features of lamellar or coarse fibrillar bone. It is thus partly immature in type, but also has areas which are highly differentiated, where one can find an indication of haversian systems being formed. In its general type the ectopic bone tissue has some features in common with the bone tissue formed in patients with osteogenesis imperfecta (see Fig. 12). In this disease the bone tissue, which is formed, does not undergo the same rebuilding which occurs normally. The formation of a compact bone tissue with haversian systems is a characteristic of normal bone tissue. In osteogenesis imperfecta, however, an immature lamellar type of bone is formed which is only partially rebuilt and thus the normal development of the bone tissue in osteogenesis imperfecta is disturbed. In the formation of ectopic bone tissue there is certainly a lack of organ differentiation and there might be a similar mechanism in operation in the case of osteogenesis imperfecta.

The mineral salt deposited in the ectopic bone, produced by the injection of alcohol into rabbit muscles, has an x-ray diffraction pattern identical with that of normal bone. The physical relationship be-

tween the organic and inorganic components seems to be identical with that in normal bone. The c-axis of the apatite unit cells being approximately parallel with the main direction of the collagenous fibrillae. The width of the x-ray diffraction lines indicate a rather low particle size similar to that found in ordinary bone.

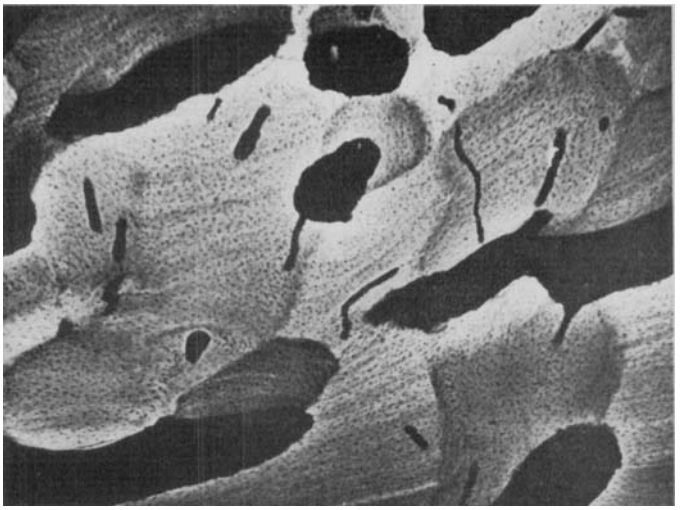

Fig. 12.
Microradiogram of compact bone tissue from a case of osteogenesis imperfecta. The "normal" appearance with haversian systems is disturbed and the lamellar form is dominating. Voltage: 22.5 kV. Filter: Be + mica (Philips diffraction tube with Cu-target. Eastman-Kodak Spectroscopic Plate 649.

The results presented above tend to indicate that ectopic bone produced in rabbit has a molecular structure and composition similar to that of ordinary rabbit bone. In vitro isotope exchange reveals no structural difference between ectopic and normal bone. The quantitative aspects of the isotope exchange have not been examined.

SUMMARY

The properties of ectopic bone produced by injecting 40 % ethanol into muscles of young rabbits have been studied by biophysical methods. X-ray absorption and diffraction techniques were used along with microscopic examinations in polarized and transmitted light. The in vitro exchange of Ca^{45} was studied by autoradiography. The ultrastructure and complexity of ectopic bone tissue as examined by these

biophysical methods show great similarities with bone tissue formed under physiological conditions in the same animals. The organization of the ectopic bone examined on the light microscopic level is altered in comparison with the mature bones performing their physiological function.

RESUME

Les propriétés de l'os ectopique produit par injection de 40 % d'éthanol dans les muscles de jeunes lapins ont été étudiées à l'aide de méthodes biophysiques. L'absorption de rayons X et la technique de la diffraction ont été utilisées au cours des examens microscopiques à la lumière polarisée et transmise. L'échange in vitro de Ca^{45} a été étudié par autoradiographie. La structure et la complexité du tissu ectopique examiné à l'aide de ces méthodes biophysiques montre de grandes similarités avec le tissue osseux formé d'après les conditions physiologiques chez les mêmes animaux. La constitution de l'os ectopique examiné à la moyenne microscopique de la lumière est altérée par comparaison avec la manière dont les os entièrement formés accomplissent leur fonction physiologique.

ZUSAMMENFASSUNG

Die Eigenschaften vom ektopischen Knochen, der mittels Injektion von 40 % Ethanol in den Muskeln von jungen Kaninchen erzeugt worden war, wurden mittels biophysikalischer Methoden untersucht. Röntgenstrahlen, Absorptions und Difraktions-Methoden wurden zusammen mit mikroskopischen Untersuchungen im polarisierten und übertragenen Licht angewendet. Der in vitro-Austausch von Ca^{45} würde mittels Autoradiographie studiert. Die Ultrastruktur und Kompliziertheit von ektopischem Knochengewebe, untersucht mit diesen biophysikalischen Methoden, zeigt grosse Ähnlichkeit mit Knochengewebe, das unter physiologischen Bedingungen in denselben Tieren entwickelt wurde. Die Organisierung des ektopischen, auf der lichtmikroskopischen Basis untersuchten Knochens ist im Vergleich mit dem reifen, seine physiologische Funktion versehenden Knochen, verändert.

REFERENCES

Chesley, R.: Rev. Sci. Instr. *18*: 422: 1947.

Engfeldt, B., Engström, A., and *Zetterström, R.:* J. Bone and Joint Surg. In the press.

Engström, A.: Acta radiol. Suppl. *63*: 1946.
– Physiol. Rev. *33*: 190: 1953.
Engström, A., and *Lindström, B.:* Nature *163*: 563: 1949.
– – Biochim. Biophys. Acta *4*: 351: 1950.
Engström, A., and *Wegstedt, L.:* Acta radiol. *35*: 345: 1951.
Heinen, J. H., Dabbs, G. H., and *Mason, H. A.:* J. Bone and Joint Surg. *31*: 765: 1949.
Lacroix, P.: Nature, London *156*: 576: 1945.
– The organization of bones. Churchill, London, 1951.
Levander, G.: Surg., Gynes. and Obst. *67*: 705: 1938.